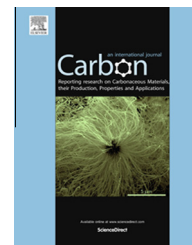


Available at www.sciencedirect.com

ScienceDirect

journal homepage: www.elsevier.com/locate/carbon

Pyrolytic carbon-coated Si nanoparticles on elastic graphene framework as anode materials for high-performance lithium-ion batteries

Fan Zhang, Xi Yang, Yuqing Xie, Ningbo Yi, Yi Huang, Yongsheng Chen *

Key Laboratory of Functional Polymer Materials and Centre of Nanoscale Science and Technology, Institute of Polymer Chemistry, College of Chemistry, Nankai University, 300071 Tianjin, China

ARTICLE INFO

Article history:

Received 11 August 2014

Accepted 20 October 2014

Available online 25 October 2014

ABSTRACT

Silicon is one of the most attractive anode materials for next-generation lithium-ion batteries, but generally it has poor cycle performance because of its severe volume change during lithiation/delithiation and its low intrinsic electrical conductivity. We fabricated a ternary Si-based composite Si@C/GF in which Si nanoparticles were coated on a thin carbon layer by pyrolysis of phenolic resin and encapsulated in a graphene framework (GF). The GF provides an elastic and robust three-dimensional structure to buffer the large volume change of Si, while the PR-pyrolytic carbon not only limits the huge volume change of Si, but also retains good contact with both the GF and Si to maintain electrode integrity. As a result, the double-protected Si nanoparticles have a much improved cycle stability (85% capacity retention, ca. 650 mAh/g after 200 cycles at 1 A/g) as well as high specific capacity and good rate performance.

© 2014 Elsevier Ltd. All rights reserved.

1. Introduction

Much effort has been made in recent years to develop high energy density rechargeable lithium-ion batteries (LIBs) and ultralong cycle life for use in electronic devices, electric vehicles, and communication equipment [1–5]. Currently, the primary commercial anode material for LIBs, graphite, cannot satisfy the demand of a high energy density due to its low theoretical capacity (372 mAh/g). Consequently, high capacity anode materials such as alloy-type anodes have been explored for the energy density improvement [6–8]. Silicon (Si) is considered to be one of the most promising anode materials owing to its highest theoretical capacity (~4200 mAh/g), low discharge potential (~0.2 V with respect to Li/Li⁺), natural abundance, etc [9–12]. Nevertheless, the main disadvantages of Si anode materials are the huge volume change (>300%)

during lithiation/delithiation and the presence of unstable surface electrolyte interphase (SEI) films, which lead to severe pulverization and the consequent loss of contact with the current collector, low cycling efficiency and rapid capacity fading [13,14]. One effective strategy to solve these issues and improve the whole electrochemical performance of Si anodes is to construct Si nanostructures, such as nanoparticles [15–17], nanowires [11,18,19], and nanotubes [20–22], which can more easily accommodate the stresses caused by the volume change than can bulk Si [23]. However, fabricating these Si nanostructures usually involves expensive and cumbersome processes such as high-temperature chemical vapor deposition (CVD) or complex chemical reactions with templates, which are not suitable for industrial production. Another effective strategy is to coat amorphous carbon [24,25] or conductive polymers [26,27] on Si, which not only

* Corresponding author: Fax: +86 2223 499992.

E-mail address: yschen99@nankai.edu.cn (Y. Chen).

<http://dx.doi.org/10.1016/j.carbon.2014.10.046>

0008-6223/© 2014 Elsevier Ltd. All rights reserved.

increase the electrical conductivity, but also limit the huge volume change of Si and thus retain the electrode integrity.

In recent years, graphene, with its unique properties such as high electrical conductivity, superior mechanical flexibility, high thermal and chemical stability, has been shown to be a good candidate for the conducting and buffering matrix in LIBs, which can greatly improve the reversible capacity, cycling stability, and rate capability [28–30]. Consequently, graphene has also been involved in Si anode materials as a robust and elastic matrix to wrap or coat Si, which can greatly improve the whole electrochemical performance [9,31–35]. However, the simple combination of graphene sheets with Si nanoparticles cannot guarantee the homogeneous dispersion of Si nanoparticles. Besides, the graphene sheets do not fully contact the Si nanoparticles especially when the Si content increases, which leads to direct contact of Si with the electrolyte and degrades the cycle stability.

Better than simply fabricating Si/graphene composites, the introduction of a second carbon phase such as graphite [36] or amorphous carbon [37,38] has been demonstrated to be another effective way to improve the cycle stability of Si anode materials. In this work, we designed a ternary Si-based composite Si@C/GF in which Si nanoparticles were coated on a thin carbon layer by pyrolysis of phenolic resin (PR) and encapsulated in a graphene framework (GF) with greatly increased cycle stability. It is worth noting that the GF provides an elastic and robust three-dimensional (3D) structure to buffer the large volume change of Si, while the amorphous PR-pyrolytic carbon not only has a high reversible capacity (about 400 mAh/g) [39], but also limits the huge volume change of Si and retains good contact with both the GF and Si to maintain electrode integrity. Hence, the composite Si@C/GF exhibits significantly enhanced electrochemical performances especially the cycle stability as an anode material in LIBs, compared to binary Si/GF composite and similar materials [37,38].

2. Experimental

2.1. Materials synthesis

2.1.1. Synthesis of graphene oxide alcogel

First, graphene oxide (GO) hydrogel was synthesized from natural flake graphite (average particle diameter of 300 μm , 99.95% purity, Qingdao Huarun Graphite Co., Ltd.) by a modified Hummers method [40], and the average size of the GO sheets was about 20 μm . It was then centrifuged (12,000 rpm, 30 min) 5 times replacing the solvent with ethanol, and finally a GO alcogel was prepared with a concentration of 5–8 mg/mL.

2.1.2. Preparation of Si-APS alcohol suspension

A Si-aminopropyltriethoxysilane (APS) alcohol suspension was prepared using a similar method to what was previously reported [41]. 1.5 g of Si nanoparticles (below 100 nm, Shanghai Chaowei Nano Science and Technology Ltd.) were dispersed in 150 mL of ethanol by sonication. After 1 h, 1.5 mL of APS was added to the above suspension and stirred at

40 °C for 24 h under a N_2 atmosphere. It was then centrifuged and dispersed in 300 mL of ethanol containing 0.3 mL HCl (36 wt%) by ultrasonication for 3 h to obtain a Si-APS alcohol suspension of 5 mg/mL.

2.1.3. Preparation of Si@C/GF composite

In a typical synthesis of Si@C/GF composite, the GO alcogel (5 mg/mL) and Si-APS alcohol suspension (5 mg/mL) were homogeneously mixed at a volume ratio of 1:2 (5 mL:10 mL) with intense agitation. Then the mixture was poured into a 25 mL Teflon-lined stainless steel autoclave and heated to 180 °C for 12 h. A GF-encapsulated Si (Si/GF) cylindrical alcogel was formed and the solvent was then exchanged from ethanol to distilled water. Phenol (31 mg, Tianjin Guangfu Fine Chemical Research Institute) and formaldehyde (44 mg, Tianjin Guangfu Fine Chemical Research Institute) were then added to the Si/GF hydrogel and a hydrothermal reaction between the two was performed at 180 °C for 12 h, during which time phenolic resin was formed. The phenolic resin-coated Si/GF hydrogel was washed and freeze-dried, and finally pyrolyzed at 800 °C for 3 h with a heating rate of 5 °C/min under a H_2/Ar (5:95 v/v) atmosphere to obtain the Si@C/GF composites. GF and Si/GF were prepared following similar method for comparison.

2.2. Characterization

Transmission electron microscopy (TEM) was performed using a JEOL TEM-2100 electron microscope operated at 200 kV. Scanning electron microscopy (SEM) was carried out using a LEO 1530 VP field emission scanning electron microscope with an acceleration voltage of 10 kV. Powder X-ray diffraction (XRD) analysis was performed on a Rigaku D/Max-2500 diffractometer with $\text{Cu K}\alpha$ radiation. Thermogravimetric (TG) measurements (Netzsch-STA 449C) were conducted from room temperature to 800 °C at a heating rate of 10 °C/min in air.

2.3. Cell fabrication and electrochemical characterization

Electrochemical measurements were carried out using coin-type cells. To prepare working electrodes, Si@C/GF composite, Super P carbon black, and poly(vinylidene fluoride) (PVDF, in N-methyl-2-pyrrolidone) with mass ratio of 80:10:10 were mixed to produce a homogeneous slurry and coated onto a 10 μm thick Cu foil. After heating at 60 °C for 3 h and 150 °C for 1 h, the electrode sheet was pressed and punched into 10 mm diameter electrodes with a mass loading of ~ 0.5 mg. The coin-type cells were assembled in an argon-filled glove box with lithium metal foil as the counter/reference electrode, and 1 M LiPF_6 in ethylenecarbonate/diethylcarbonate/vinylene carbonate (1:1:0.02 v/v/v) as the electrolyte. The additive vinylene carbonate has been proved for better cycling performance [42]. The charge/discharge measurements were performed using a battery test system (LAND CT2001A model, Wuhan LAND Electronics. Ltd.) over a voltage window from 0.01 to 2 V at room temperature. Electrochemical impedance spectral measurements were recorded using an Autolab system (Metrohm) in the frequency range from 100 kHz to 10 mHz.

3. Results and discussion

A schematic of the fabrication of the Si@C/GF composite is shown in Fig. 1. First, Si/GF was prepared from 20 μm graphene oxide (GO) sheets and APS-decorated Si nanoparticles by a solvothermal reaction. The GF has an elastic and robust structure (shown in Fig. S1 in supporting information), which can buffer the large volume change of Si. To further improve the cycle stability, amorphous PR-pyrolytic carbon was also introduced and coated on the Si/GF by an in-situ hydrothermal reaction followed by annealing to form Si@C/GF.

By using the solvothermal reaction and high-temperature annealing, both Si/GF and Si@C/GF are formed as cylindrical aerogels (shown in the insets of Fig. 2a and d, respectively). It can be seen that the color of Si/GF is gray while Si@C/GF is black due to the further coating of PR-pyrolytic carbon. The structure of Si/GF and Si@C/GF composites was characterized by SEM and TEM (Fig. 2). Both composites exhibit a 3D cross-linked porous structure (Fig. 2a and d), mainly attributed to the GF forming a 3D skeleton (Fig. S2). Fig. 2b and c show magnified SEM images of Si/GF, in which a large amount of Si nanoparticles embedded in the wrinkled graphene sheets can be observed, with a few Si nanoparticles partially exposed at the outer surface. Fig. 2e and f show magnified SEM images of Si@C/GF, in which fewer Si nanoparticles can be observed compared to Si/GF, and the Si nanoparticles have become totally wrapped in many more wrinkled and crumpled graphene/carbon sheets. No obvious PR-pyrolytic carbon can be distinguished from the graphene sheets, which may be because the PR has polymerized on the surfaces of Si/GF during the hydrothermal polymerization process, forming more wrinkled thin-layer carbon sheets. Different from the previous reports of Si/graphene/C composites [37,38], our ternary composite Si@C/GF shows a 3D cross-linked porous structure, which would be more beneficial for fast ion transportation and good rate performance. Besides, the PR-pyrolytic carbon

can also exhibit a highly reversible capacity (about 400 mAh/g) [39] and excellent cycling performance, thus improving the whole electrochemical performance by two mechanisms.

The microstructure of Si@C/GF can be clearly observed in the TEM images shown in Fig. 2g–i. It can be seen that many Si nanoparticles (~ 100 nm) are embedded in the wrinkled sheets with the morphology similar to that of graphene (Fig. 2g and h). These wrinkled sheets may probably be graphene sheets cross-linked with some amorphous carbon sheets. Notably, Fig. 2i shows that the Si nanoparticle is coated with a thin uniform layer of amorphous carbon of 2 nm in thickness (a thin layer of amorphous silicon oxide can also be observed, which is probably due to the oxidation of Si nanoparticles during fabrication). Therefore, the Si nanoparticles between the graphene and the amorphous carbon layers are double-protected.

Fig. S3a shows the XRD patterns of the as-prepared products GF, Si/GF and Si@C/GF, together with that of the pristine Si nanoparticles. The peaks of the Si/GF and Si@C/GF composites are identical with those of the Si nanoparticles, indicating that the Si nanoparticles are still crystalline both in Si/GF and Si@C/GF. The diffraction patterns of GF can also be observed in both Si/GF and Si@C/GF, which illustrates that the 3D structure of GF are still maintained in these materials. Diffraction from the amorphous carbon is hardly observed in Si@C/GF, mainly due to the low amount in the composites. To quantify the amounts of graphene and PR-based amorphous carbon, thermogravimetric analysis (TGA) was conducted in air and the curves are shown in Fig. S3b. As the oxidation of the Si in air causes a mass increase to be 104.1 wt%, the contents of Si in Si/GF and Si@C/GF composites can be calculated to be 81.9 wt% and 65 wt%, respectively. Accordingly, the content of graphene in the Si/GF composite is about 18.1 wt%, and the total amount of graphene and amorphous carbon in Si@C/GF is about 35 wt%. Considering that the Si@C/GF

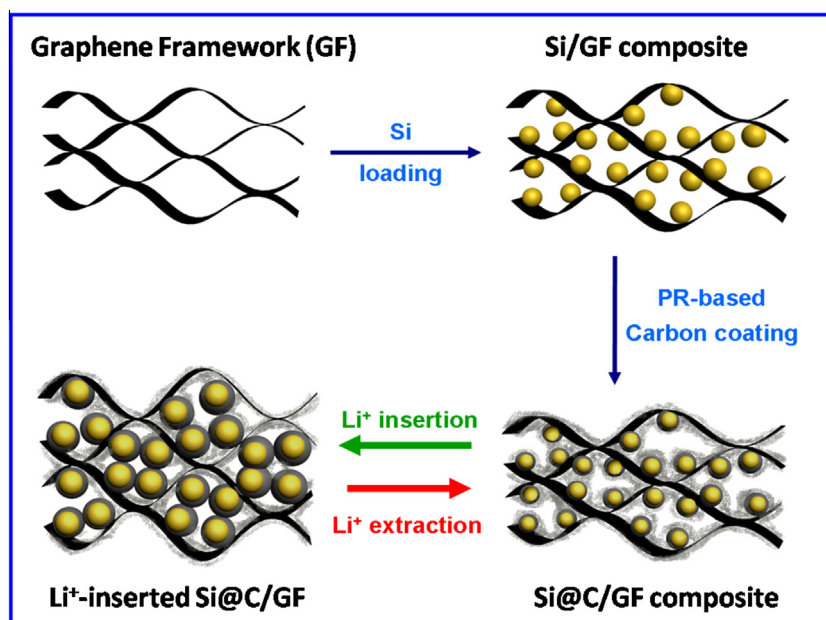


Fig. 1 – Schematic of the fabrication of the Si@C/GF composite. (A color version of this figure can be viewed online.)

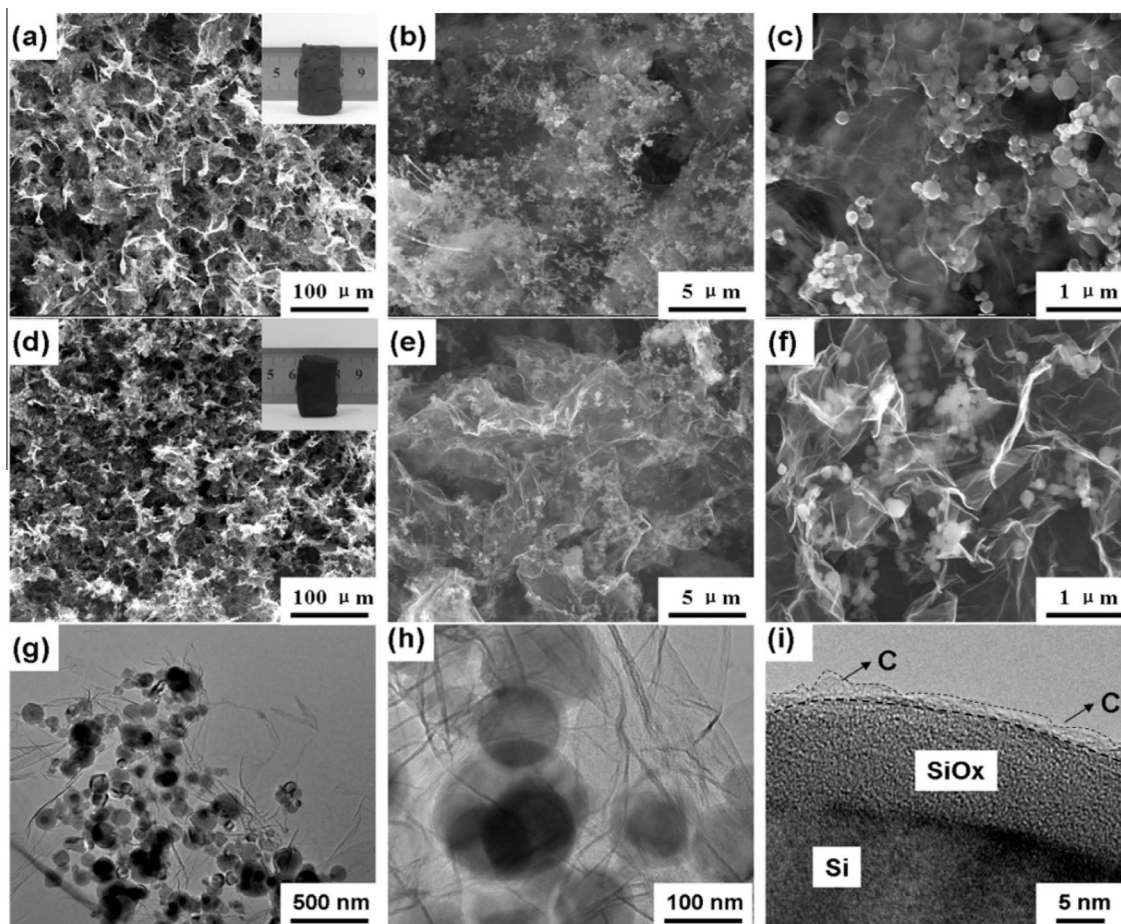


Fig. 2 – (a–c) SEM images of binary composite Si/GF; (d–f) SEM images of ternary composite Si@C/GF; (g–i) TEM images of Si@C/GF.

composite is prepared by coating a layer of PR-based amorphous carbon on the Si/GF composite, where the mass ratio of Si to graphene is 81.9:18.1, the amounts of graphene and amorphous carbon in Si@C/GF are calculated to be about 14.4 wt% and 20.6 wt%, respectively.

From the above results we can demonstrate that the Si@C/GF composites are made of Si nanoparticles, graphene frameworks and amorphous carbon, where the Si nanoparticles are well embedded in the 3D graphene framework, and are also coated by a thin uniform amorphous carbon layer. The graphene framework and the amorphous carbon coating layers have a double-protection mechanism, which can provide both a sufficient conductive, porous and elastic network for facilitating electron/ion transfer, buffering the deformation stresses, preventing aggregation and pulverization of Si nanoparticles, and also maintaining a stable structure during the Li^+ insertion/extraction process. Thus, such a unique structure of Si@C/GF would be expected to have superior performance for lithium storage.

The electrochemical performance of the Si@C/GF composite was investigated using half cells vs. Li/Li^+ in the potential range 0.01–2 V, as shown in Fig. 3. Fig. 3a shows the charge-discharge profiles of the Si@C/GF for the first three cycles at a current density of 0.1 A/g. The first discharge and charge capacities are as high as 4976 mAh/g and 3062 mAh/g,

respectively (the capacity values are calculated based on the total mass of Si@C/GF), corresponding to an initial Coulombic efficiency of 61.5%. The unusual high initial discharge specific capacity of the composites and lower initial Coulombic efficiency may be caused by some side reactions with electrolytes and the formation of a solid electrolyte interphase (SEI) film on the surface of the Si nanoparticles [11,43] which may be due to the high surface area of the graphene and the small amount of amorphous carbon [44,45] in the first cycle, thus resulting in the excessive consumption of Li^+ and irreversible capacity. However, the Coulombic efficiency exceeds 90% in the second and third cycles, and the charge capacities in the second and third cycles are 3010 mAh/g and 2956 mAh/g respectively, showing almost no degradation, indicating high reversible capacities. Fig. 3b and c show the rate performance of Si@C/GF, Si/GF, Si nanoparticles, and GF. It can be clearly seen that the composite Si@C/GF exhibits good rate capability and maintains a high specific capacity in the current density range of 0.1–1.5 A/g, while the Si nanoparticles show dramatic decay and the GF has a low specific capacity despite having excellent rate capability. The discharge specific capacity of Si@C/GF is 2956, 1955, 1264, 830, and 715 mAh/g at the current density of 0.1, 0.2, 0.5, 1, and 1.5 A/g, respectively. The volumetric capacity of the Si@C/GF electrode is estimated to be $\sim 1176 \text{ mAh/cm}^3$ at 0.2 A/g (see supporting information for

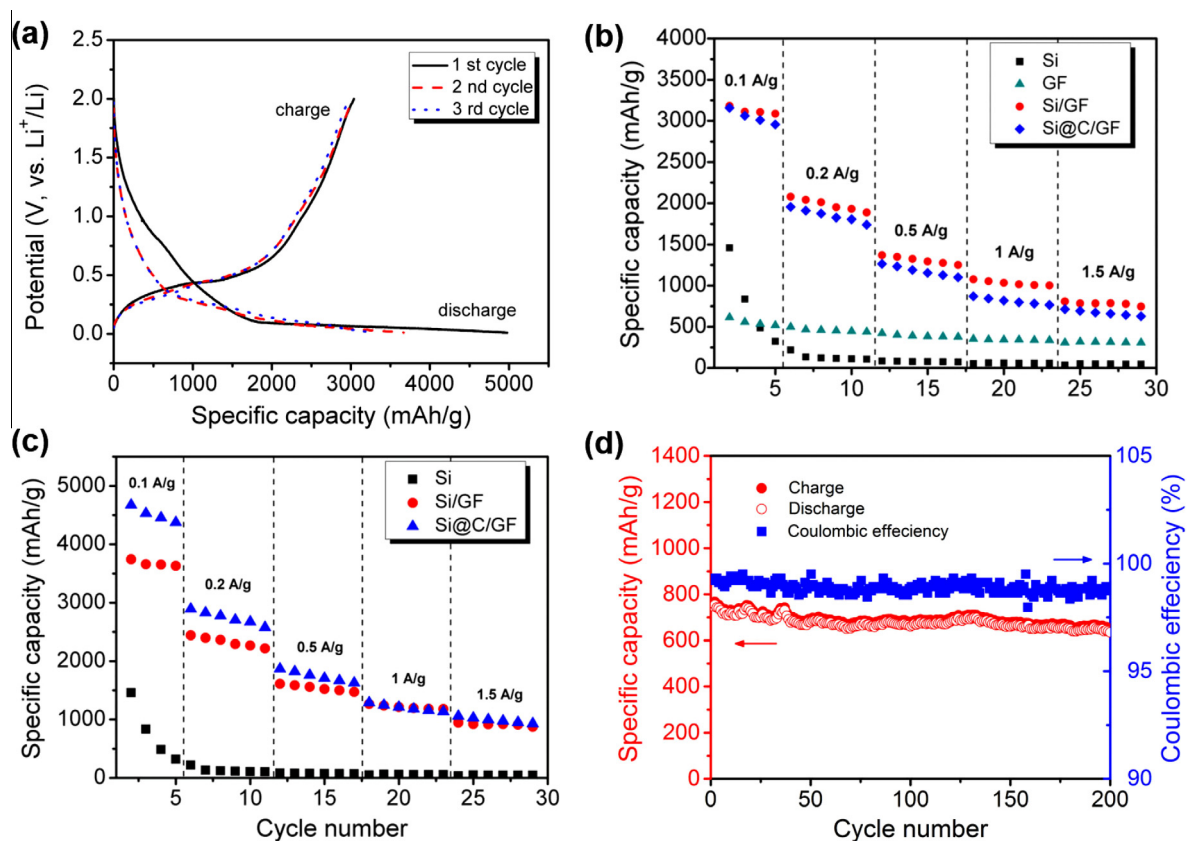


Fig. 3 – Electrochemical performance of the Si@C/GF composite. (a) First three voltage–capacity profiles of the Si@C/GF at a current density of 0.1 A/g; (b) charge (delithiation) capacities of Si, Si/GF and Si@C/GF at various rates based on the total active electrode material weight; (c) charge (delithiation) capacities of Si, Si/GF and Si@C/GF at various rates based on the Si weight; (d) cycling performance and Coulombic efficiency of the Si@C/GF at 1 A/g for 200 cycles. (A color version of this figure can be viewed online.)

calculation details), which is about twice of graphite electrode ($\sim 620 \text{ mAh/cm}^3$) [46]. The composite Si/GF shows a little higher specific capacity than that of Si@C/GF, which is due to the more Si content in Si/GF. However, when the specific capacities were calculated on the basis of the Si mass (Fig. 3c), the Si@C/GF gives higher specific capacities than Si/GF especially at low current densities, which indicates that the presence of Si in Si@C/GF contributes more than it does in Si/GF. In addition, the specific capacity of Si@C/GF also remains very stable in subsequent cycles, which has a value of $\sim 650 \text{ mAh/g}$ with 85.1% retention after 200 cycles especially at the high current density of 1 A/g (Fig. 3d), much higher than the theoretical specific capacity of the graphite (372 mAh/g). Besides, the Coulombic efficiency also remains nearly 100% in every cycle. These results indicate that a stable SEI film is formed and the stable electrical contact of Si is retained during cycling despite the drastic volume change, leading to good cycle stability of the composite.

For comparison, the cycle stability of the Si@C/GF and Si/GF composites was also investigated under the same electrochemical conditions. As illustrated in Fig. 4a, Si@C/GF shows much better cycle performance than Si/GF. After cycling for 200 cycles at 1 A/g, the specific capacity of the Si@C/GF electrode remains at 85.1%, while the value for the Si/GF electrode

is only 42.6%. It is worthy to note that even at the same content of Si ($\sim 65 \text{ wt\%}$), the Si@C/GF composite still exhibits better cycle performance (85% retention) than the binary composite (68% retention), indicating the important function of the carbon layer during the electrochemical reactions (see Fig. S4 in the supporting information). The capacity retention value of Si@C/GF is also much higher than the similar reported studies [37,38], where there is only $\sim 68\%$ retention after 100 cycles, thus demonstrating the better cycle stability of our Si@C/GF. Fig. 4b shows Nyquist plots of the Si/GF and Si@C/GF electrodes. Both impedance curves show a compressed semicircle in the high-frequency region and an inclined line in the low-frequency region, which can be assigned to the charge-transfer resistance and semi-diffusion of lithium ions into the Si respectively [47,48]. Obviously, the diameter of the semicircle for the Si@C/GF electrode is much smaller than that for the Si/GF electrode (see the inset plot), which means that the Si@C/GF electrode has a lower resistance for the interfacial electrochemical reaction, indicating the improved conductivity and the more stable structure of Si@C/GF.

All the above results demonstrate that the amorphous carbon layers play a crucial role in improving the cycle stability of the Si@C/GF, because they can not only coat the

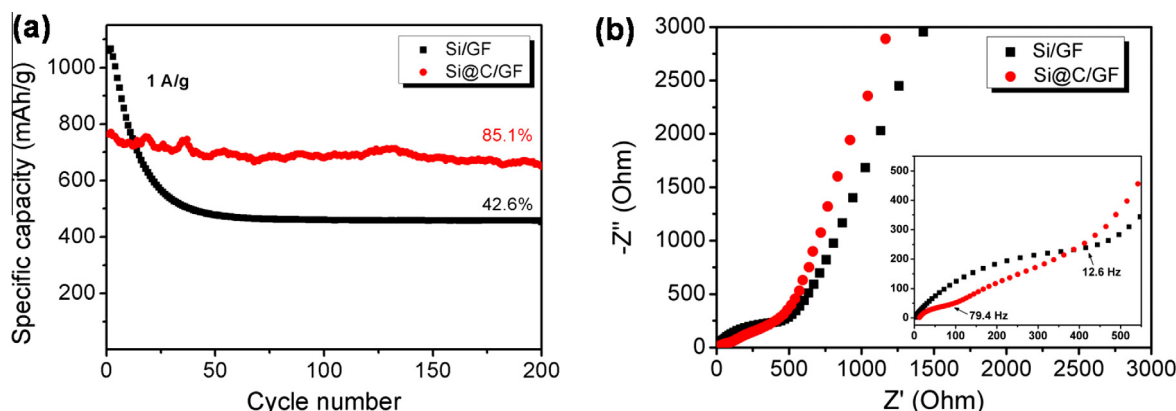


Fig. 4 – (a) Cycling performance of Si/GF and Si@C/GF at a current density of 1 A/g; (b) Nyquist plots of Si/GF and Si@C/GF. (A color version of this figure can be viewed online.)

Si nanoparticles to alleviate the effects of volume changes, but also connect with the graphene framework to construct a more rigid network thus stabilizing the structure while also improving the conductivity. Therefore, our results clearly demonstrate the important role of the well-organized interleaved structure of Si@C/GF in improving the electrochemical performance.

4. Conclusion

We have described a novel method for the synthesis of a graphene framework and amorphous carbon double-protected Si nanoparticles to enhance the electrochemical performance of lithium-ion batteries. The Si@C/GF material was prepared by the solvothermal reaction of graphene oxide and Si nanoparticles and further coating by amorphous carbon layers using phenolic resin as the carbon precursor. The as-prepared material shows a significantly improved lithium-storage performance in terms of highly reversible lithium-storage capacity, good rate capability and excellent cycle stability, compared to Si/GF and the bare Si nanoparticles. The Si@C/GF also shows much better cycle performance than other similar Si/graphene/C composites. Therefore, this strategy, which uses elastic graphene framework as the supporting network for loading Si nanoparticles, and amorphous carbon as the coating layer, is demonstrated to be an effective way to improve the cycling performance of Si-based anode materials.

Acknowledgements

The authors gratefully acknowledge the financial supports from MOST (2012CB933401 and 2014CB643502), NSFC (51273093, 21374050, and 51373078), PCSIRT (IRT1257) and Tianjin city (13RCGFGX01121).

Appendix A. Supplementary data

Supplementary data associated with this article can be found, in the online version, at <http://dx.doi.org/10.1016/j.carbon.2014.10.046>.

REFERENCES

- [1] Tarascon JM, Armand M. Issues and challenges facing rechargeable lithium batteries. *Nature* 2001;414:359–67.
- [2] Dunn B, Kamath H, Tarascon JM. Electrical energy storage for the grid: a battery of choices. *Science* 2011;334:928–35.
- [3] Ji X, Lee KT, Nazar LF. A highly ordered nanostructured carbon–sulphur cathode for lithium–sulphur batteries. *Nat Mater* 2009;8:500–6.
- [4] Wu XL, Jiang LY, Cao FF, Guo YG, Wan LJ. LiFePO₄ nanoparticles embedded in a nanoporous carbon matrix: superior cathode material for electrochemical energy-storage devices. *Adv Mater* 2009;21:2710–4.
- [5] Armand M, Tarascon JM. Building better batteries. *Nature* 2008;451:652–7.
- [6] Zhang WJ. A review of the electrochemical performance of alloy anodes for lithium-ion batteries. *J Power Sources* 2011;196:13–24.
- [7] Park CM, Kim JH, Kim H, Sohn HJ. Li-alloy based anode materials for Li secondary batteries. *Chem Soc Rev* 2010;39:3115–41.
- [8] Wu H, Cui Y. Designing nanostructured Si anodes for high energy lithium ion batteries. *Nano Today* 2012;7:414–29.
- [9] Wang B, Li XL, Zhang XF, Luo B, Jin MH, Liang MH, et al. Adaptable silicon carbon nanocables sandwiched between reduced graphene oxide sheets as lithium ion battery anodes. *ACS Nano* 2013;7:1437–45.
- [10] Magasinski A, Dixon P, Hertzberg B, Kvit A, Ayala J, Yushin G. High-performance lithium-ion anodes using a hierarchical bottom-up approach. *Nat Mater* 2010;9:353–8.
- [11] Chan CK, Peng H, Liu G, Mcilwrath K, Zhang XF, Huggins RA, et al. High-performance lithium battery anodes using silicon nanowires. *Nat Nanotechnol* 2008;3:31–5.
- [12] Su X, Wu QL, Li JC, Xiao XC, Lott A, Lu WQ, et al. Silicon-based nanomaterials for lithium-ion batteries: a review. *Adv Energy Mater* 2013. <http://dx.doi.org/10.1002/aenm.201300882>.
- [13] Li H, Wang Z, Chen L, Huang X. Research on advanced materials for li-ion batteries. *Adv Mater* 2009;21:4593–607.
- [14] Wu H, Chan G, Choi JW, Ryu I, Yao Y, McDowell MT, et al. Stable cycling of double-walled silicon nanotube battery anodes through solid-electrolyte interphase control. *Nat Nanotechnol* 2012;7:310–5.
- [15] Bao ZH, Weatherspoon MR, Shian S, Cai Y, Graham PD, Allan SM, et al. Chemical reduction of three-dimensional silica micro-assemblies into microporous silicon replicas. *Nature* 2007;446:172–5.

- [16] Kim H, Han B, Choo J, Cho J. Three-dimensional porous silicon particles for use in high-performance lithium secondary batteries. *Angew Chem Int Ed* 2008;47:10151–4.
- [17] Ge M, Rong J, Fang X, Zhang A, Lu Y, Zhou C. Scalable preparation of porous silicon nanoparticles and their application for lithium-ion battery anodes. *Nano Res* 2013;6:174–81.
- [18] Chan CK, Patel RN, O'Connell MJ, Korgel BA, Cui Y. Solution-grown silicon nanowires for lithium-ion battery anodes. *ACS Nano* 2010;4:1443–50.
- [19] Cui LF, Yang Y, Hsu CM, Cui Y. Carbon-silicon core-shell nanowires as high capacity electrode for lithium ion batteries. *Nano Lett* 2009;9:3370–4.
- [20] Park MH, Kim MG, Joo J, Kim K, Kim J, Ahn S, et al. Silicon nanotube battery anodes. *Nano Lett* 2009;9:3844–7.
- [21] Yoo JK, Kim J, Jung YS, Kang K. Scalable fabrication of silicon nanotubes and their application to energy storage. *Adv Mater* 2012;24:5452–6.
- [22] Kasavajjula U, Wang C, Appleby AJ. Nano- and bulk-silicon-based insertion anodes for lithium-ion secondary cells. *J Power Sources* 2007;163:1003–39.
- [23] Yu Y, Gu L, Zhu C, Tsukimoto S, Aken PA, Maier J. Reversible storage of lithium in silver-coated three-dimensional macroporous silicon. *Adv Mater* 2010;22:2247–50.
- [24] Hu YS, Demir-Cakan R, Titirici MM, Müller JO, Schlögl R, Antonietti M, et al. Superior storage performance of a Si@SiO_x/C nanocomposite as anode material for lithium-ion batteries. *Angew Chem Int Ed* 2008;47:1645–9.
- [25] Yin YX, Xin S, Wan LJ, Li CJ, Guo YG. Electro spray synthesis of silicon/carbon nanoporous microspheres as improved anode materials for lithium-ion batteries. *J Phys Chem C* 2011;115:14148–54.
- [26] Wu H, Yu GH, Pan LJ, Liu N, McDowell MT, Bao ZN, et al. Stable Li-ion battery anodes by in-situ polymerization of conducting hydrogel to conformally coat silicon nanoparticles. *Nat Commun* 2013;4:1943–8.
- [27] Liu G, Xun SH, Vukmirovic N, Song XY, Olalde-Velasco P, Zheng HH, et al. Polymers with tailored electronic structure for high capacity lithium battery electrodes. *Adv Mater* 2011;23:4679–83.
- [28] Wu ZS, Ren WC, Wen L, Gao LB, Zhao JP, Chen ZP, et al. Graphene anchored with Co₃O₄ nanoparticles as anode of lithium ion batteries with enhanced reversible capacity and cyclic performance. *ACS Nano* 2010;4:3187–94.
- [29] Yang X, Zhang L, Zhang F, Huang Y, Chen YS. Sulfur-infiltrated graphene-based layered porous carbon cathodes for high-performance lithium-sulfur batteries. *ACS Nano* 2014;8:5208–15.
- [30] Wang HL, Cui LF, Yang Y, Casalongue HS, Robinson JT, Liang Y, et al. Mn₃O₄-graphene hybrid as a high-capacity anode material for lithium ion batteries. *J Am Chem Soc* 2010;132:13978–80.
- [31] Ji JY, Ji HX, Zhang LL, Zhao X, Bai X, Fan XB, et al. Graphene-encapsulated Si on ultrathin-graphite foam as anode for high capacity lithium-ion batteries. *Adv Mater* 2013;25:4673–7.
- [32] Lee JK, Smith KB, Hayner CM, Kung HH. Silicon nanoparticles-graphene paper composites for Li ion battery anodes. *Chem Commun* 2010;46:2025–7.
- [33] Xin X, Zhou XF, Wang F, Yao XY, Xu XX, Zhu YM, et al. A 3D porous architecture of Si/graphene nanocomposite as high-performance anode materials for Li-ion batteries. *J Mater Chem* 2012;22:7724–30.
- [34] Park SH, Kim HK, Ahn DJ, Lee SI, Roh KC, Kim KB. Self-assembly of Si entrapped graphene architecture for high-performance Li-ion batteries. *Electrochem Commun* 2013;34:117–20.
- [35] Chang JB, Huang XK, Zhou GH, Cui SM, Hallac PB, Jiang JW, et al. Multilayered Si nanoparticle/reduced graphene oxide hybrid as a high-performance lithium-ion battery anode. *Adv Mater* 2014;26:758–64.
- [36] Gan L, Guo HJ, Wang ZX, Li XH, Peng WJ, Wang JX, et al. A facile synthesis of graphite/silicon/graphene spherical composite anode for lithium-ion batteries. *Electrochim Acta* 2013;104:117–23.
- [37] Zhou M, Cai TW, Pu F, Chen H, Wang Z, Zhang HY, et al. Graphene/carbon-coated Si nanoparticle hybrids as high-performance anode materials for Li-ion batteries. *ACS Appl Mater Interfaces* 2013;5:3449–55.
- [38] Li H, Lu CX, Zhang BP. A straightforward approach towards Si@C/graphene nanocomposite and its superior lithium storage performance. *Electrochim Acta* 2014;120:96–101.
- [39] Wang MS, Fan LZ. Silicon/carbon nanocomposite pyrolyzed from phenolic resin as anode materials for lithium-ion batteries. *J Power Sources* 2013;244:570–4.
- [40] Becerril HA, Mao J, Liu ZF, Stoltenberg RM, Bao ZN, Chen YS. Evaluation of solution-processed reduced graphene oxide films as transparent conductors. *ACS Nano* 2008;2:463–70.
- [41] Zhou M, Pu F, Wang Z, Cai TW, Chen H, Zhang HY, et al. Facile synthesis of novel Si nanoparticles-graphene composites as high-performance anode materials for Li-ion batteries. *Phys Chem Chem Phys* 2013;15:11394–401.
- [42] Chen L, Wang K, Xie X, Xie J. Effect of vinylene carbonate (VC) as electrolyte additive on electrochemical performance of Si film anode for lithium ion batteries. *J. Power Sources* 2007;174:538–43.
- [43] Graetz J, Ahn CC, Yazami R, Fultz B. Highly reversible lithium storage in nanostructured silicon. *Electrochem Solid-State Lett* 2003;6:A194–7.
- [44] Wang G, Shen X, Yao J, Park J. Graphene nanosheets for enhanced lithium storage in lithium ion batteries. *Carbon* 2009;47:2049–53.
- [45] Liang M, Zhi L. Graphene-based electrode materials for rechargeable lithium batteries. *J Mater Chem* 2009;19:5871–8.
- [46] Kovalenko I, Zdyrko B, Magasinski A, Hertzberg B, Milicev Z, Burtovyy R, et al. A major constituent of brown algae for use in high-capacity Li-ion batteries. *Science* 2011;333:75–9.
- [47] Zhou X, Yin YX, Wan LJ, Guo YG. Facile synthesis of silicon nanoparticles inserted into graphene sheets as improved anode materials for lithium-ion batteries. *Chem Commun* 2012;48:2198–200.
- [48] Yang S, Li G, Zhu Q, Pan Q. Covalent binding of Si nanoparticles to graphene sheets and its influence on lithium storage properties of Si negative electrode. *J Mater Chem* 2012;22:3420–5.